Performance analysis of VLC systems with multi-color light sources beyond RGB LEDs

Borja Genoves Guzman, *Member, IEEE*, and Alexis A. Dowhuszko, *Senior Member, IEEE*

***Abstract*—Visible light communication (VLC) is being considered as a solution to reinforce the indoor wireless communication services provided so far almost exclusively over radio frequency bands. Multi-color light-emitting diodes (LEDs) are convenient light sources in this context, which can multiply the number of data streams with the aid of wavelength division multiplexing while providing an aggregate white light that is suitable for illumination. Although Red-Green-Blue (RGB) is the most popular combination considered in the literature for tri-color LEDs, other *less explored* options can also be considered to reach different illumination and communication key performance indicators in VLC systems. To carry out this analysis, an exact closed-form procedure is derived in this paper for the allocation of power per individual LED chip for *any* tri-color combination, which is beyond the state-of-art of the approximated methods used so far. The most convenient tri-color LED combination is also identified for providing communication and illumination services at different correlated color temperatures (CCTs). While RedOrange-Green-Blue is the most energy-efficient tri-color LED combination for illumination (in lm/W), RedOrange-Cyan-Blue is the most convenient tri-color combination to maximize the spectral efficiency for communication (in bps/Hz/W).**

***Index Terms*—Multi-color LED, optical wireless communication, power allocation, RGB, visible light communication.**

I. Introduction

Visible light communication (VLC) has been drawing the attention of the research community for more than a decade, showing its potential to satisfy the ever-increasing demand of wireless data traffic indoors [1]. The possibility of achieving high *data rates* with high levels of *security* at a relatively *low cost* makes VLC a promising technology to complement the wireless services provided so far almost exclusively over radio frequency (RF) bands. In addition, since VLC uses wireless signals in a region of the electromagnetic spectrum that is visible to humans, its high emitted optical power can be reused for illumination while offering a *feeling of security* as any eavesdropper should be located around the small-sized spotlight in which the legitimate user is placed.

VLC makes use of a light-emitting diode (LED) as transmitter and a photodiode (PD) as receiver. The data-carrying signal modulates the intensity of the current that drives the LED, and the fraction of this emitted optical power that reaches the sensitive area of the PD in the receiver is transformed into an electrical signal. Thus, the transmission and reception of data in a VLC system follows an intensity modulation with direct detection (IM/DD) scheme. Since VLC simultaneously provides illumination and data communication services [2], an aggregate light beam – that should resemble a single white light source for the *human eye* – must be created to fulfill the existing indoor illumination standards. There are two main LED technologies that can be used for this purpose: phosphor-converted LEDs (PC-LEDs) and multi-color LEDs [3]. PC-LED technology is widespread due to its low complexity, affordable cost, and good color rendering index (CRI) [4]. In contrast, multi-color LEDs are more complex but offer characteristics that are very valuable for communications, such as the provision of a higher electrical modulation bandwidth per color chip [5], the compatibility with wavelength division multiplexing (WDM) [6], and the chance to mitigate co-channel interference from external light sources and/or adjacent VLC access points (APs) with the aid of optical filters and a proper network planning [7], [8].

The optical power emitted by each color chip affects the correlated color temperature (CCT) of the multi-color LED [4], which is a metric that distinguishes the hue of the white light that is generated for illumination. As it will be shown later, the CCT affects the communication and power consumption key performance indicators (KPIs) of a VLC system based on multi-color LEDs. Few works in the literature have studied the VLC performance when using Red-Green-Blue (RGB) LEDs under illumination constraints. For example, the authors of [9]–[11] proposed an optimization problem for the optical power allocation satisfying illumination and communication requirements. Similarly, Jian *et al.* focused on optimizing the sum-rate of a multi-user system rather than optimizing the power consumption [12], whereas Gong *et al.* studied an optimal symbol modulation power allocation scheme when considering a multi-color LED in point-to-point and broadcast communication systems [13]. However, all these papers relied on inappropriate methods for defining the allocation of power on the multiple color LEDs of the VLC system: They computed the target white color as a linear combination of individual color coordinates [14] or luminous fluxes [12], [15], [16], which may lead to inaccurate results as it will be shown.

Differently, we propose an alternative power allocation method for multi-color VLC systems that follows the steps to compute the chromaticity coordinates of a light source. We consider the use of tri-chromatic LEDs, as it is the most extended technology to generate white light when combining multiple LED colors; however, we highlight the necessity of exploring other tri-color LED combinations different from the conventional RGB, which is typically chosen to create the

B. Genoves Guzman is with the Electrical and Computer Engineering Department, University of Virginia, Charlottesville, VA 22904 USA (e-mail: bgenoves@virginia.edu) and with affiliation in Signal Theory and Communications Department, University Carlos III of Madrid, 28911 Spain.

A. Dowhuszko is with the Department of Information and Communications Engineering, Aalto University, 02150 Espoo, Finland (e-mail: alexis.dowhuszko@aalto.fi).

widest possible palette of colors as perceived by the human eye in screens and monitors. Nevertheless, there are many other tri-color LED combinations that allow obtaining a white light in the Planckian locus, which contains the coordinates in the chromaticity diagram that are suitable for illumination, ranging from warm to cool white light. These *other* tri-color LED combinations are unexplored in the context of VLC systems, and they have potential to offer better illumination and/or communication performance. Our method starts from the approximation of the actual spectral power emission of a color LED reported in [17], continues with the computation of the tri-stimulus values in closed form, and ends with the determination of the chromaticity coordinates of the aggregate white light emitted by the tri-color LED. Such new power allocation method, which is precise by definition, can be used to optimize both illumination and data communication KPIs of VLC systems based on tri-color LEDs. Optimizing an illumination KPI is beneficial for applications where the light intensity and hue are critical, such as smart indoor agriculture [18]. Optimizing a communication KPI, in contrast, is convenient to provide spectral-efficient VLC services with an aggregate white light that is suitable for indoor illumination according to standards.

When compared to the state-of-art research reported in the literature, this paper presents the following contributions:

- A closed-form expression to compute the CIE 1931 tri-stimulus values (X, Y, Z) and (x, y) chromaticity coordinates of a single-color LED is derived. This formula, which depends on values that can be easily extracted from any LED data sheet (e.g., peak and half-maximum power wavelengths, luminous efficacy, etc.), enables theoretical studies in VLC systems based on tri-color LEDs.
- For the first time, a generalized power allocation method to *precisely* achieve a target white light hue of a VLC systems using *any* tri-color LED combination is presented.
- The tri-color LED combinations that optimize the energy consumption (lm/W) and the data rate efficiency (bps/Hz/W) of a VLC system are studied. These KPIs are relevant to optimize the illumination and communication services. *Unexplored* tri-color combinations that offer better illumination and communication KPIs than traditional RGB LEDs are also noted.
- For the sake of practicality, this work evaluates four tri-color LED combinations that ensure obtaining all possible points in the Planckian locus by allocating properly the transmit power among the individual LED chips. This provides an aggregate light that spans from warm (CCT $=$ 2700 K) to cool (CCT $=$ 6500 K) white light. However, the proposed method is not restricted to the studied tri-color LED combinations and can be used with other tri-color combinations selected by the VLC system designer, even with LED chips provided by different manufacturers.

The rest of this paper is structured as follows: Section II introduces the system model, including the closed-form formulas that approximate the spectral power emission of a single-color LED, the color matching functions, and the communication KPIs. Section III derives the closed-form expressions of the proposed exact power allocation method that generates an aggregate white light at a desired CCT in the Planckian locus of the CIE 1931 chromaticity diagram. Section IV shows the simulation results and carries out the performance analysis. Finally, conclusions are drawn in Section V.

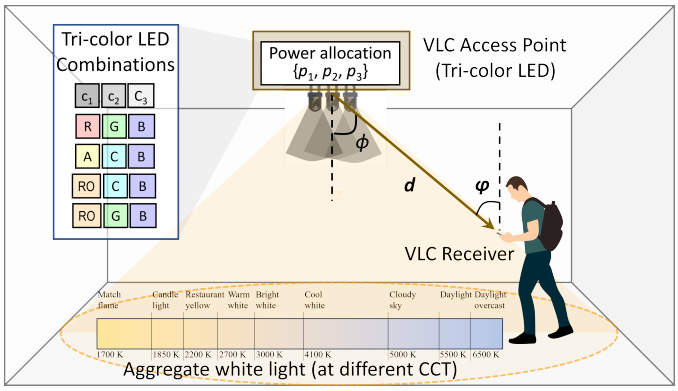

Fig. 1. Indoor VLC system using tri-color LED technology. The target white-light hue, measured in the form of a Correlated Color Temperature (CCT), is a result of the mixing of three single colored light beams coming from the individual LED chips. The illumination and communication KPIs depend on the power allocated (p_1, p_2, p_3) and selected LED color such as Red (R), Green (G), Blue (B), Amber (A), Cyan (C) and RedOrange (RO).

II. System Model

Consider the VLC scenario presented in Fig. 1, consisting of a tri-color LED that generates white light by the proper mixing of three single-color light sources with an aggregate optical power spectra given by $p_{\mathrm{o}}(\lambda) = p_{\mathrm{o},c_1}(\lambda) + p_{\mathrm{o},c_2}(\lambda) + p_{\mathrm{o},c_3}(\lambda)$, where $p_{\mathrm{o},c_1}(\lambda)$, $p_{\mathrm{o},c_2}(\lambda)$, $p_{\mathrm{o},c_3}(\lambda)$ are the optical power spectra for the individual LED color chips with indexes c_1, c_2 and c_3, respectively. All color sensations that are visible to a person with average eyesight are included in the well-known CIE 1931 chromaticity diagram [19]. The (x, y) coordinates in the CIE 1931 chromaticity diagram are computed as [20]

$$x = \frac{X}{X+Y+Z}, \quad y = \frac{Y}{X+Y+Z}, \tag{1}$$

where (X, Y, Z) are the tri-stimulus values for a given optical power spectrum $p_{\mathrm{o}}(\lambda)$, and they represent the response of the three kinds of cone cells that serve as photoreceptors in the human eye. The tri-stimulus values are determined using [20]

$$X = \int_{\lambda_1}^{\lambda_2} \overline{x}(\lambda)\, p_{\mathrm{o}}(\lambda)\, \mathrm{d}\lambda, \tag{2}$$

$$Y = \int_{\lambda_1}^{\lambda_2} \overline{y}(\lambda)\, p_{\mathrm{o}}(\lambda)\, \mathrm{d}\lambda, \tag{3}$$

$$Z = \int_{\lambda_1}^{\lambda_2} \overline{z}(\lambda)\, p_{\mathrm{o}}(\lambda)\, \mathrm{d}\lambda, \tag{4}$$

where λ is the wavelength in nanometers (nm). Note that, in these formulas, the visible light spectrum is defined between $\lambda_1 = 380$ nm and $\lambda_2 = 780$ nm. Moreover, $\overline{x}(\lambda)$, $\overline{y}(\lambda)$, and $\overline{z}(\lambda)$ stand for the CIE XYZ color matching functions (CMFs), also known as the average spectral responses of each kind of cone cells. We now introduce the expressions to approximate

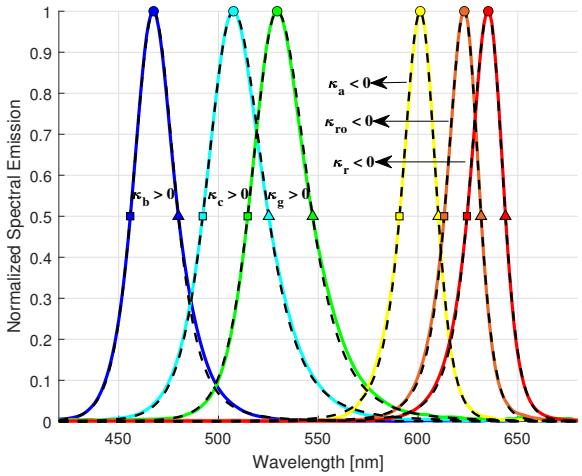

Fig. 2. Measured spectrum (solid lines) and asymmetric Pearson-VII approximation (dashed lines) when the DC-bias current of the LEDs is 200 mA [17]. Spectral emissions of LEDs from left to right: Blue (B), Cyan (C), Green (G), Amber (A), RedOrange (RO), and Red (R). Peak wavelength $\lambda_{\mathrm{p},c}$ and half-maximum wavelengths $\lambda^{(1)}_{0.5,c}$ and $\lambda^{(2)}_{0.5,c}$ are marked with circles, squares and triangles, respectively. Skewness shown with the sign of Kurtosis index κ_c.

TABLE I
PARAMETERS TO APPROXIMATE THE EMITTED OPTICAL SPECTRAL POWER FOR THE LUXEON REBEL COLOR LEDS USED IN THIS PAPER.

Color	**Sub-Index**	**Central Wavelength**	**Left half max. wavel.**	**Right half max. wavel.**	**Skewness**
	c	$\lambda_{\mathrm{p},c}$ [nm]	$\lambda^{(1)}_{0.5,c}$ [nm]	$\lambda^{(2)}_{0.5,c}$ [nm]	κ_c
Blue	'b'	467.5	455.8	479.9	Positive
Cyan	'c'	507.5	492.1	525.2	Positive
Green	'g'	529.4	514.6	547.2	Positive
Amber	'a'	601.1	590.7	610.2	Negative
RedOrange	'ro'	623.2	613.1	631.6	Negative
Red	'r'	635.2	624.5	643.8	Negative

the optical power spectra of single-color LEDs and the CMFs in closed form to derive our performance analysis.

A. Proposed Closed-Form Approximation for the Optical Spectral Power Density of a single Color LED — $p_{\mathrm{o},c}(\lambda)$

Based on [17], we assume that the normalized emitted optical spectra of a color LED c can be accurately approximated as an asymmetric Pearson-VII distribution, i.e.,

$$p_{\mathrm{o},c}(\lambda) = \left(1 + \frac{\left(\lambda - \lambda_{\mathrm{p},c}\right)^2}{W_c\left[1 + m_c\,\mathrm{sign}(\lambda - \lambda_{\mathrm{p},c})\right]}\right)^{-S_c(\lambda)}, \quad (5)$$

where

$$W_c = \frac{W_c^{(2)} + W_c^{(1)}}{2}, \qquad m_c = \frac{W_c^{(2)} - W_c^{(1)}}{W_c^{(2)} + W_c^{(1)}}, \quad (6)$$

are the width and asymmetric coefficients of the spectral power distribution, respectively, with

$$W_c^{(2)} = \frac{\left(\lambda^{(2)}_{0.5,c} - \lambda_{\mathrm{p},c}\right)^2}{2^{1/S_c(\lambda^{(2)}_{0.5,c})} - 1}, \quad W_c^{(1)} = \frac{\left(\lambda^{(1)}_{0.5,c} - \lambda_{\mathrm{p},c}\right)^2}{2^{1/S_c(\lambda^{(1)}_{0.5,c})} - 1}. \quad (7)$$

The shape parameter of the optical spectral power density

TABLE II
COEFFICIENTS OF THE LINEAR COMBINATION OF ASYMMETRIC GAUSSIAN DISTRIBUTIONS USED TO APPROXIMATE THE CIE 1931 COLOR MATCHING FUNCTIONS $\overline{x}(\lambda)$, $\overline{y}(\lambda)$, AND $\overline{z}(\lambda)$.

	Gauss. term $g_{k,l}(\lambda)$	Coefficient $a_{k,l}$	Mode $\mu_{k,l}$	Std. Dev. (1) $\sigma^{(1)}_{k,l}$	Std. Dev. (2) $\sigma^{(2)}_{k,l}$
$\widetilde{x}(\lambda)$	$g_{1,1}(\lambda)$	1.056	599.8	37.9	31.0
	$g_{1,2}(\lambda)$	0.362	442.0	16.0	26.7
	$g_{1,3}(\lambda)$	−0.065	501.1	20.4	26.2
$\widetilde{y}(\lambda)$	$g_{2,1}(\lambda)$	0.821	568.8	46.9	40.5
	$g_{2,2}(\lambda)$	0.286	530.9	16.3	31.1
$\widetilde{z}(\lambda)$	$g_{3,1}(\lambda)$	1.217	437.0	11.8	36.0
	$g_{3,2}(\lambda)$	0.681	459.0	26.0	13.8

of the LED with color index c is given by

$$S_c(\lambda) = 3 - \mathrm{sign}(\lambda_{\mathrm{p},c} - \lambda), \qquad \text{for } \kappa_c < 0, \quad (8)$$

where the negative skewness (κ_c) refers to a longer (or fatter) tail on the left side of the distribution. Otherwise,

$$S_c(\lambda) = 3 - \mathrm{sign}(\lambda - \lambda_{\mathrm{p},c}), \qquad \text{for } \kappa_c > 0. \quad (9)$$

The *skewness*, which in this example is equivalent to the third standardized moment of random variable λ, is given by

$$\kappa_c = \frac{\mathbb{E}\{(\lambda - \mathbb{E}\{\lambda\})^3\}}{\left[\mathbb{E}\{(\lambda - \mathbb{E}\{\lambda\})^2\}\right]^{3/2}}, \quad (10)$$

where $\mathbb{E}\{\lambda\} = \int_{\lambda_1}^{\lambda_2} \lambda\, f(\lambda)\,\mathrm{d}\lambda$, in which $f(\lambda)$ represents the probability density function of λ. Therefore, we have a negative skewness in the case of the optical spectral power distribution for the Red (R), RedOrange (RO), and Amber (A) LEDs. The opposite situation happens when the skewness is positive, which means that the right-hand side tail is longer than the left-hand side one, such as in the case of the optical spectral power distribution for the Green (G), Cyan (C), and Blue (B) LEDs. Fig. 2 represents the measured and approximated spectral optical power emissions for each color considering *LUXEON Rebel* color LED part numbers. The required points for drawing the approximated spectra with the closed-form expressions introduced in [17] are also highlighted in the figure. The values of these key parameters are summarized in Table I for the different color LEDs.

B. Proposed Closed-Form Approximation for the Color Matching Functions — $\overline{x}(\lambda)$, $\overline{y}(\lambda)$, and $\overline{z}(\lambda)$

The values that the CIE 1931 CMFs $\overline{x}(\lambda)$, $\overline{y}(\lambda)$, and $\overline{z}(\lambda)$ take for different wavelengths λ in the visible light region have been experimentally determined by the International Commission for Illumination and its standardized tabulated values can be found in the literature [21]. However, to derive a closed-form formula that approximates the tri-stimulus values corresponding to a color LED based on the parameters reported in Table I, we use the approximations for the CIE 1931 CMFs that are presented in [22], which take the form of

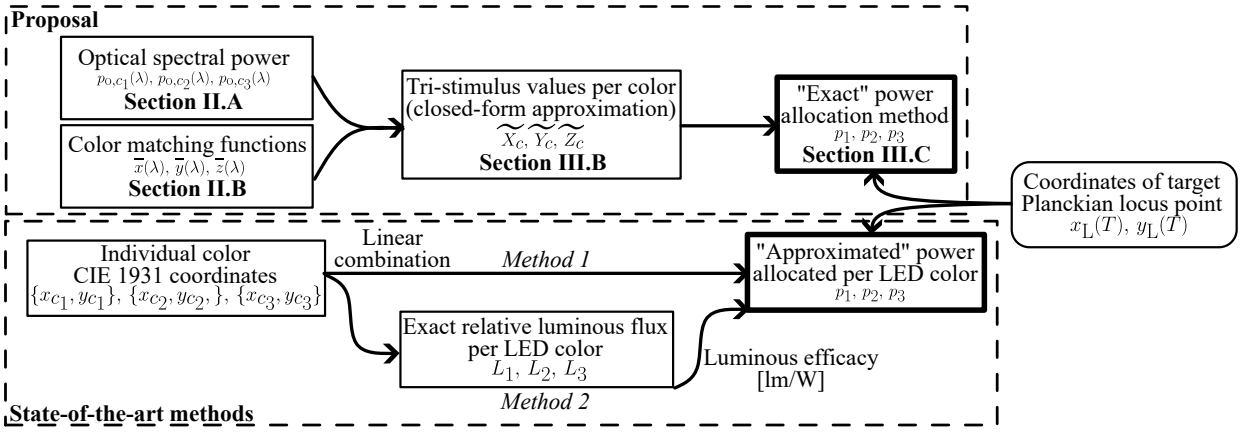

Fig. 3. Block diagram that compares state-of-the-art methods reported in the literature with the new proposed method for optical power allocation in VLC systems based on tri-color LEDs. The two state-of-the-art methods used for comparisons in this paper are *Method 1* [14] and *Method 2* [12], [15], [16].

multiple piece-wise continuous Gaussian functions, i.e.,

$$\widetilde{x}(\lambda)=a_{1,1}\,g\big(\lambda;\mu_{1,1},\sigma_{1,1}^{(1)},\sigma_{1,1}^{(2)}\big)+a_{1,2}\,g\big(\lambda;\mu_{1,2},\sigma_{1,2}^{(1)},\sigma_{1,2}^{(2)}\big)+a_{1,3}\,g\big(\lambda;\mu_{1,3},\sigma_{1,3}^{(1)},\sigma_{1,3}^{(2)}\big), \tag{11}$$

$$\widetilde{y}(\lambda)=a_{2,1}\,g\big(\lambda;\mu_{2,1},\sigma_{2,1}^{(1)},\sigma_{2,1}^{(2)}\big)+a_{2,2}\,g\big(\lambda;\mu_{2,2},\sigma_{2,2}^{(1)},\sigma_{2,2}^{(2)}\big), \tag{12}$$

$$\widetilde{z}(\lambda)=a_{3,1}\,g\big(\lambda;\mu_{3,1},\sigma_{3,1}^{(1)},\sigma_{3,1}^{(2)}\big)+a_{3,2}\,g\big(\lambda;\mu_{3,2},\sigma_{3,2}^{(1)},\sigma_{3,2}^{(2)}\big), \tag{13}$$

where the asymmetric Gaussian function attains the form

$$g\big(\lambda;\mu_{k,l},\sigma_{k,l}^{(1)},\sigma_{k,l}^{(2)}\big)=g_{k,l}(\lambda)=\begin{cases}\exp\Big(-\frac{(\lambda-\mu_{k,l})^2}{2\left(\sigma_{k,l}^{(1)}\right)^2}\Big), & \lambda<\mu_{k,l},\\ \exp\Big(-\frac{(\lambda-\mu_{k,l})^2}{2\left(\sigma_{k,l}^{(2)}\right)^2}\Big), & \lambda\geq\mu_{k,l},\end{cases} \tag{14}$$

and the coefficients of equations (11), (12) and (13) are shown in Table II.

C. Key Performance Indicators for VLC-based Communication

For the sake of simplicity, in this paper we consider that all the chips of the tri-color LED emit the same data stream. This is equivalent to assuming that there is no optical power leakage that may generate inter-stream interference when WDM is applied. Thus, although the equivalent channel model for the tri-color VLC system under analysis can be considered as a 3×3 MIMO system, we are currently not exploiting the possibility of applying MIMO precoding in transmission to maximize the aggregate data rate of a multi-stream transmission based on wavelength-division multiplexing. Furthermore, since the communication takes place over visible light, we must ensure that the resulting aggregate (white) light that is generated has its color coordinates on the Planckian locus of the CIE 1931 chromaticity diagram to make it suitable for illumination. To achieve this, we apply a power allocation method between the LED chips of the tri-color combination as detailed in Section III. Thus, although the equivalent VLC channel model can be represented as a 3×3 matrix regardless of the tri-color LED combination that is used, every particular case will provide a different set of channel gain coefficients in the different positions of the square matrix. Each tri-color combination must be considered separately because each color LED has different characteristics for both communication and illumination, as it will be shown later, which leads to a different system performance that deserves to be studied separately. In this situation, the electrical received power of the output of the photodetector can be formulated as

$$P_{\rm elec,rx}=\left(H\int_{\lambda_1}^{\lambda_2}\eta(\lambda)\delta(\lambda)\big[p_{{\rm o},c_1}(\lambda)+p_{{\rm o},c_2}(\lambda)+p_{{\rm o},c_3}(\lambda)\big]{\rm d}\lambda\right)^2, \tag{15}$$

where $\eta(\lambda)$ is the spectral responsivity of the photodetector [A/W] and $\delta(\lambda)$ is the spectral transmittance of the optical filter, whereas the free-space optical channel [23] is

$$H=\frac{A_{\rm pd}(m+1)}{2\pi d^2}\cos^m(\phi)\cos(\varphi), \tag{16}$$

where $A_{\rm pd}$ [m] is the active sensitive area of the photodetector, $m=-1/\log_2\big(\cos(\phi_{1/2})\big)$ is the Lambertian index of the LED that characterizes the directivity of the light beam, in which $\phi_{1/2}$ [rad] is the half-power semi-angle of the LED, and d [m] is the Euclidean distance between the LED and photodetector. For the sake of simplicity, we assume that all color LEDs have the same Lambertian index m. Parameters ϕ [rad] and φ [rad] are the irradiance and incidence angles, as shown in Fig. 1. The total noise power produced at the receiver of the VLC link can be modeled as a combination of shot and thermal noise, attaining the form

$$P_{\rm N}=\big(2q\sqrt{P_{\rm elec,rx}}+(4\,\kappa_B\,T_{\rm abs})/R_{\rm L}\big)\,F_{\rm s}, \tag{17}$$

where $q=1.6\cdot10^{-19}$ [C] is the electrical charge of the electron, $\kappa_B=1.38\times10^{-23}$ [J/K] is the Boltzmann constant, $T_{\rm abs}$ [K] is the absolute temperature in Kelvin, $R_{\rm L}$ [Ω] is the equivalent load resistance of the receiver circuit, and $F_{\rm s}$ [Hz] is the sampling frequency which depends on the symbol rate. Then, the spectral efficiency for an IM/DD VLC system can be formulated as [24]

$$\gamma=\frac{1}{2}\log_2\left(1+\frac{\exp(1)}{2\pi}\frac{P_{\rm elec,rx}}{P_{\rm N}}\right)\quad[{\rm bit/s/Hz}], \tag{18}$$

where SNR $=P_{\rm elec,rx}/P_{\rm N}$ is the signal-to-noise power ratio (SNR) of the electrical signal at the output of the

photodetector.

III. Proposed Exact Method for Power Allocation

This section presents an exact power allocation method for any tri-color LED combination. For this, we first introduce an overview of the proposal and then we derive the closed-form formula to compute the tri-stimulus of the color LEDs, to be used in our new proposed *exact* method for power allocation.

A. Overview of the New Proposed Method for Power Allocation of VLC Systems Based on Tri-Color LEDs

Fig. 3 presents the block diagram that compares the new proposed method with state-of-the-art *Method 1* [14] and *Method 2* [12], [15], [16]. These prior methods rely on the linear combinations of CIE 1931 chromaticity coordinates of individual color LEDs to compute the power allocation, overlooking the actual optical power spectra of the LEDs. As it will be shown later, this may lead to inaccurate results in some of the tri-color LED combinations under analysis. In our proposal, to come up with a suitable optical power allocation that achieves the target chromaticity coordinates (or CCT) of the aggregate white light, we carry out the following steps:

1) Firstly, the optical power spectral density for a color LED $p_{\mathrm{o},c}(\lambda)$ is modeled in closed form using three key parameters that can be easily obtained from the data sheet of the LED [17]. These parameters are the peak wavelength ($\lambda_{\mathrm{p},c}$), the left- and right-side half-maximum wavelengths ($\lambda^{(1)}_{0.5,c}$ and $\lambda^{(2)}_{0.5,c}$), and the skewness (κ_c). This is part of previous literature [17] and is introduced in Section II-A. Besides, we need the closed-form approximations for the CMFs that appear in Section II-B.
2) Secondly, analytical approximations for the tri-stimulus values $(\widetilde{X}_c, \widetilde{Y}_c, \widetilde{Y}_c)$ that corresponds to the light emitted by each individual color LED are derived. This point is addressed in the following Section III-B.
3) Finally, the procedure to identify the optical power allocation per color LED to reach the target white light chromaticity (or CCT) is presented. For this, a system with three linear equations and three variables is solved. This point is addressed in the following Section III-C.

B. Closed-Form Computation of single Color LED Tri-Stimulus Values

To find a closed-form approximation for the tri-stimulus values that corresponds to a given color LED with index c, we plug (11)-(13) into equations (2)-(4) to obtain

$$\widetilde{X}_c = \int_{\lambda_1}^{\lambda_2} \widetilde{x}(\lambda)\, p_{\mathrm{o},c}(\lambda)\, \mathrm{d}\lambda = I_{1,1} + I_{1,2} + I_{1,3}, \quad (19)$$

$$\widetilde{Y}_c = \int_{\lambda_1}^{\lambda_2} \widetilde{y}(\lambda)\, p_{\mathrm{o},c}(\lambda)\, \mathrm{d}\lambda = I_{2,1} + I_{2,2}, \quad (20)$$

$$\widetilde{Z}_c = \int_{\lambda_1}^{\lambda_2} \widetilde{z}(\lambda)\, p_{\mathrm{o},c}(\lambda)\, \mathrm{d}\lambda = I_{3,1} + I_{3,2}, \quad (21)$$

where

$$I_{k,l} = a_{k,l} \int_{\lambda_1}^{\lambda_2} g\big(\lambda; \mu_{k,l}, \sigma^{(1)}_{k,l}, \sigma^{(2)}_{k,l}\big)\, p_{\mathrm{o},c}(\lambda)\, \mathrm{d}\lambda \quad (22)$$

can be expanded as three definite integrals whose integration bounds are defined according to the values taken by the peak wavelength $\lambda_{\mathrm{p},c}$ of LED spectral power and the mode $\mu_{k,l}$ of the asymmetric Gaussian component used to approximate the corresponding CMF. Then, when $\lambda_{\mathrm{p},c} \le \mu_{k,l}$,

$$\begin{aligned} I_{k,l} =& a_{k,l} \int_{\lambda_1}^{\lambda_{\mathrm{p},c}} \exp\Big(-\frac{(\lambda-\mu_{k,l})^2}{2\left(\sigma^{(1)}_{k,l}\right)^2}\Big)\Big(1+\frac{\left(\lambda-\lambda_{\mathrm{p},c}\right)^2}{W_1}\Big)^{-S_1} \mathrm{d}\lambda \\ &+ a_{k,l} \int_{\lambda_{\mathrm{p},c}}^{\mu_{k,l}} \exp\Big(-\frac{(\lambda-\mu_{k,l})^2}{2\left(\sigma^{(1)}_{k,l}\right)^2}\Big)\Big(1+\frac{\left(\lambda-\lambda_{\mathrm{p},c}\right)^2}{W_2}\Big)^{-S_2} \mathrm{d}\lambda \\ &+ a_{k,l} \int_{\mu_{k,l}}^{\lambda_2} \exp\Big(-\frac{(\lambda-\mu_{k,l})^2}{2\left(\sigma^{(2)}_{k,l}\right)^2}\Big)\Big(1+\frac{\left(\lambda-\lambda_{\mathrm{p},c}\right)^2}{W_2}\Big)^{-S_2} \mathrm{d}\lambda. \quad (23) \end{aligned}$$

On the other hand, when $\mu_{k,l} < \lambda_{\mathrm{p},c}$, we have

$$\begin{aligned} I_{k,l} =& a_{k,l} \int_{\lambda_1}^{\mu_{k,l}} \exp\Big(-\frac{(\lambda-\mu_{k,l})^2}{2\left(\sigma^{(1)}_{k,l}\right)^2}\Big)\Big(1+\frac{\left(\lambda-\lambda_{\mathrm{p},c}\right)^2}{W_1}\Big)^{-S_1} \mathrm{d}\lambda \\ &+ a_{k,l} \int_{\mu_{k,l}}^{\lambda_{\mathrm{p},c}} \exp\Big(-\frac{(\lambda-\mu_{k,l})^2}{2\left(\sigma^{(2)}_{k,l}\right)^2}\Big)\Big(1+\frac{\left(\lambda-\lambda_{\mathrm{p},c}\right)^2}{W_1}\Big)^{-S_1} \mathrm{d}\lambda \\ &+ a_{k,l} \int_{\lambda_{\mathrm{p},c}}^{\lambda_2} \exp\Big(-\frac{(\lambda-\mu_{k,l})^2}{2\left(\sigma^{(2)}_{k,l}\right)^2}\Big)\Big(1+\frac{\left(\lambda-\lambda_{\mathrm{p},c}\right)^2}{W_2}\Big)^{-S_2} \mathrm{d}\lambda. \quad (24) \end{aligned}$$

Note that in (23) and (24), we have used $W_1 = W_c(1-m_c)$ and $W_2 = W_c(1+m_c)$ to simplify the notation. In addition, both equations are composed by three definite integrals over non-overlapping integration ranges, each of them of the form

$$\begin{aligned} I\big(x; [x_1, x_2], [\mu, \sigma], [x_{\mathrm{p}}, W, S]\big) \;=\; & \\ \int_{x_1}^{x_2} \exp\Big(-\frac{(x-\mu)^2}{2\,\sigma^2}\Big)\Big(1+\frac{\left(x-x_{\mathrm{p}}\right)^2}{W}\Big)^{-S} \mathrm{d}x, & \quad (25) \end{aligned}$$

where $[x_1, x_2]$ are the integration range defined according to the individual definite integrals in (23) and (24), $[\mu, \sigma]$ define the parameters of the asymmetric Gaussian component of the CMF approximation with sub-index (k, l), and $[x_{\mathrm{p}}, W, S]$ specify the parameters of the Pearson-VII function that is used to approximate the spectral power emission of the color LED.

We then apply the variable substitution $u = (x-\mu)/\sigma$ in (25) with $u_{\mathrm{p}} = (x_{\mathrm{p}} - \mu)/\sigma$, $u_1 = (x_1-\mu)/\sigma$, $u_2 = (x_2-\mu)/\sigma$, and $W_{\mathrm{p}} = W/\sigma^2$. After that, the Taylor series for the Gaussian function

$$\exp\Big(-\frac{x^2}{2}\Big) = \sum_{k=0}^{\infty} \frac{1}{k!}\Big(-\frac{x^2}{2}\Big)^k \quad (26)$$

is utilized, where $k!$ denotes the factorial of k, to obtain

$$\begin{aligned} I\big(u; [u_1, u_2], [u_{\mathrm{p}}, W_{\mathrm{p}}, S]\big) \;=\; & \\ = \int_{u_1}^{u_2} \exp\Big(-\frac{u^2}{2}\Big)\Big(1+\frac{\left(u-u_{\mathrm{p}}\right)^2}{W_{\mathrm{p}}}\Big)^{-S}(\sigma)\, du & \\ = \int_{u_1}^{u_2} \sum_{k=0}^{\infty} \frac{(-1)^k\, u^{2k}}{2^k\, k!}\Big(1+\frac{\left(u-u_{\mathrm{p}}\right)^2}{W_{\mathrm{p}}}\Big)^{-S}(\sigma)\, du. & \quad (27) \end{aligned}$$

Then, after applying a second substitution of variables using $v = (u-u_{\mathrm{p}})/\sqrt{W_{\mathrm{p}}}$ in (27) with $v_1 = (u_1-u_{\mathrm{p}})/\sqrt{W_{\mathrm{p}}}$ and

TABLE III
TRI-STIMULUS VALUES AND CIE 1931 CHROMATICITY COORDINATES WHEN USING THE ACTUAL (MEASURED) LED SPECTRAL POWER EMISSION WITH THE TABULATED CMFS AND THE DERIVED FORMULA BASED ON THE PEARSON-VII APPROXIMATION FOR THE COLOR LED OPTICAL SPECTRUM [17].

Color (index)	**Measured tri-stimulus values**			**Approximated tri-stimulus values**			**Measured coordinates**	**Approximated coordinates**	**Step MacAdam (Euclidean dist.)**
	X_c	Y_c	Z_c	$\widetilde{X}_c$	$\widetilde{Y}_c$	$\widetilde{Z}_c$	(x_c, y_c)	$(\widetilde{x}_c, \widetilde{y}_c)$	
Blue ('b')	5.7025	3.1052	35.8088	5.5589	3.0488	35.5383	(0.1278 0.0696)	(0.1259, 0.0691)	3.5 (0.0020)
Cyan ('c')	3.1026	20.1586	8.9505	3.4174	20.3230	8.7400	(0.0963 0.6258)	(0.1052, 0.6257)	2.8 (0.0089)
Green ('g')	9.6671	31.5004	2.2305	9.3236	31.2323	2.3711	(0.2228, 0.7258)	(0.2172, 0.7276)	1.8 (0.0058)
Amber ('a')	23.0832	14.5455	0.0190	22.9691	14.7068	0.0028	(0.6131, 0.3864)	(0.6096, 0.3903)	3.2 (0.0053)
RedOrange ('ro')	17.5603	8.1740	0.0046	17.5700	8.1274	0.0001	(0.6822, 0.3176)	(0.6837, 0.3163)	1.1 (0.0020)
Red ('r')	13.5377	5.7706	0.0016	13.6697	5.6915	0.0000	(0.7011, 0.2988)	(0.7060, 0.2940)	3.8 (0.0070)

$v_2 = (u_2 - u_\mathrm{p})/\sqrt{W_\mathrm{p}}$, we get the following expression:

$$
\begin{aligned}
&I\big(v;\big[v_1, v_2\big], \big[u_\mathrm{p}, W_\mathrm{p}, S\big]\big) = \\
&= \sum_{k=0}^{\infty} \frac{(-1)^k}{2^k\, k!} \int_{v_1}^{v_2} \big(\sqrt{W_\mathrm{p}} v + u_\mathrm{p}\big)^{2k} \big(1+v^2\big)^{-S} (\sigma\sqrt{W_\mathrm{p}})\, dv \\
&= \sum_{k=0}^{\infty} \frac{(-1)^k}{2^k\, k!} \int_{v_1}^{v_2} \sum_{l=0}^{2k} \binom{2k}{l} \big(\sqrt{W_\mathrm{p}} v\big)^l \big(u_\mathrm{p}\big)^{2k-l} \\
&\times \big(1+v^2\big)^{-S} (\sigma\sqrt{W_\mathrm{p}})\, dv \\
&= \sum_{k=0}^{\infty} \frac{(-1)^k}{2^k\, k!} \sum_{l=0}^{2k} \binom{2k}{l} u_\mathrm{p}^{2k-l}\, W_\mathrm{p}^{\frac{l+1}{2}} \sigma \int_{v_1}^{v_2} (v)^l \big(1+v^2\big)^{-S} dv, \quad (28)
\end{aligned}
$$

where the latter expression is obtained after re-arranging the terms when applying the binomial theorem, i.e.,

$$
\big(x+y\big)^n = \sum_{k=0}^{n} \binom{n}{k} x^{n-k}\, y^k, \quad \binom{n}{k} = \frac{n!}{(n-k)!\, k!}. \quad (29)
$$

Finally, the definite integrals of the form $\int_{v_1}^{v_2} \frac{v^l}{(1+v^2)^S} dv$ are obtained with the aid of the following recursive closed-form expressions borrowed from well-known reference books of Integrals, Series and Products [25], i.e.,

$$
\begin{aligned}
\int \frac{x^m\, dx}{(1+x^2)^n} &= -\frac{1}{2n-m-1} \frac{x^{m-1}}{(1+x^2)^{n-1}} \\
&+ \frac{m-1}{2n-m-1} \int \frac{x^{m-2} dx}{(1+x^2)^n}, \quad (30)
\end{aligned}
$$

that is valid for most values of $m \geq 2$ and $n \geq 2$, with

$$
\int \frac{x\, dx}{(1+x^2)^n} = \frac{1}{2-2n} \frac{1}{(1+x^2)^{n-1}} \quad (31)
$$

for $m = 1$ and $n \geq 2$ and

$$
\int \frac{x\, dx}{(1+x^2)} = \frac{1}{2} \ln\big(1+x^2\big) \quad (32)
$$

when $m = 1$ and $n = 1$. Similarly, when $m = 0$ and $n \geq 2$,

$$
\int \frac{dx}{(1+x^2)^n} = \frac{1}{2n-2} \frac{x}{(1+x^2)^{n-1}} + \frac{2n-3}{2n-2} \int \frac{dx}{(1+x^2)^{n-1}}, \quad (33)
$$

with

$$
\int \frac{dx}{(1+x^2)} = \arctan(x) \quad (34)
$$

when $m = 0$ and $n = 1$. Note that the recursive equation (30) does not work when $m = 2n-1$. Due to that, the following closed-form expression is used when $n = 2$ and $m = 3$, i.e.,

$$
\int \frac{x^3}{(1+x^2)^2} dx = \frac{1 + \big(1+x^2\big) \ln\big(1+x^2\big)}{2\big(1+x^2\big)}, \quad (35)
$$

and when $n = 4$ and $m = 7$, i.e.,

$$
\int \frac{x^7}{(1+x^2)^4} dx = \frac{18x^4 + 27x^2 + 11 + 6\big(1+x^2\big)^3 \ln(1+x^2)}{12\big(1+x^2\big)^3}. \quad (36)
$$

The formula for the definite integral when $n = 3$ and $m = 5$ is not included as it is not required in this analysis. Finally, combining the closed-form expressions in (28)-(36), we can obtain a recursive formula to compute the tri-stimulus values $(\widetilde{X}_c, \widetilde{Y}_c, \widetilde{Z}_c)$ per color LED, as defined in (19)-(21).

In order to avoid convergence problems when using, in *practice*, a finite number of terms to approximate the Taylor series expansion in (26), the following bound are defined for the closed-form computation of the integrals in (19)-(21), i.e.,

$$
\left.\begin{aligned}
\lambda_1 &= \max\big(\lambda_\mathrm{p} - 4\Delta^{(1)}, \mu - 3\sigma^{(1)}, 380\big) \\
\lambda_2 &= \min\ \big(\lambda_\mathrm{p} + 8\Delta^{(2)}, \mu + 3\sigma^{(2)}, 780\big)
\end{aligned}\right\} \text{ when } \kappa_c > 0, \quad (37)
$$

and

$$
\left.\begin{aligned}
\lambda_1 &= \max\big(\lambda_\mathrm{p} - 8\Delta^{(1)}, \mu - 3\sigma^{(1)}, 380\big) \\
\lambda_2 &= \min\ \big(\lambda_\mathrm{p} + 4\Delta^{(2)}, \mu + 3\sigma^{(2)}, 780\big)
\end{aligned}\right\} \text{ when } \kappa_c < 0, \quad (38)
$$

where $\Delta^{(1)} = \lambda_\mathrm{p} - \lambda_{0.5}^{(1)}$ and $\Delta^{(2)} = \lambda_{0.5}^{(2)} - \lambda_\mathrm{p}$ are the width of the spectral emission at half of its maximum amplitude, also known as full width at half maximum (FWHM), that corresponds to the left- and right-hand side tails of the asymmetric Pearson-VII function in (5) that approximates the spectral emission of the color LED. Note that (37) and (38) are justified as follows: In a Gaussian distribution $g(x)$, almost all its density is found within three standard deviations σ from the mean/mode μ; i.e., $\int_{-3\sigma}^{3\sigma} g(x)\, \mathrm{d}x \approx 0.9973$. Similarly, when studying the spectral power emission of a color LED with positive skewness (i.e., $\kappa > 0$), most of the emitted optical power is concentrated within four and eight FWHM units of the left-hand side (light) and right-hand side (heavy) tails of the asymmetric Pearson-VII approximation, i.e., $\int_{\lambda_\mathrm{p}-4\Delta^{(1)}}^{\lambda_\mathrm{p}+8\Delta^{(2)}} p_\mathrm{o}(\lambda)\, \mathrm{d}\lambda = 0.9946$. The same situation takes place when the spectral power emission of the color LED has negative skewness (i.e., $\kappa < 0$).

Table III summarizes the key parameters of the single color LEDs under analysis in the following form: 1) the *exact* measured coordinates $\big(x_c, y_c\big)$, computed experimentally with the actual optical power spectrum measured with a

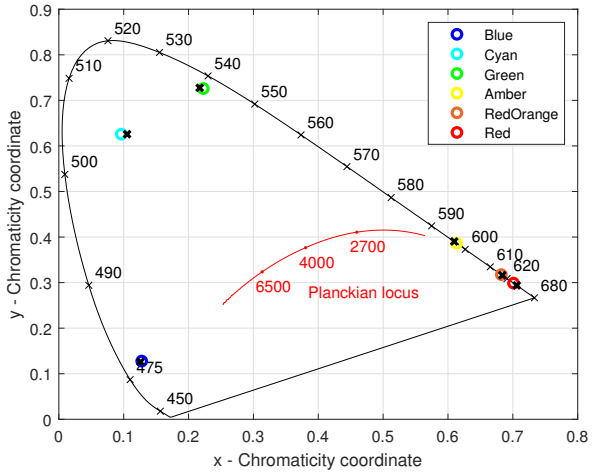

Fig. 4. Positions of the (x, y)-coordinates that corresponds to the optical power emission of the LUXEON rebel LEDs under analysis (CIE 1931). Colored circles: Values computed with actual LED emission spectra (DC-bias current = 200 mA) and tabulated color matching functions. Black markers with crosses: Values computed with the proposed closed-form method. Solid line: Planckian locus for the aggregate white light with different target CCTs.

spectrophotometer when the forward current is 200 mA [17], and using the actual tabulated CMF $\overline{x}(\lambda)$, $\overline{y}(\lambda)$ and $\overline{z}(\lambda)$ with the Simpson's 1/3 rule for numerical integration to compute the exact tri-stimulus values; 2) the closed-form *approximated* coordinates $(\widetilde{x}_c, \widetilde{y}_c)$ when using $p_{\mathrm{o},c}(\lambda)$ for the spectral emission of the color LED and $\widetilde{x}(\lambda)$, $\widetilde{y}(\lambda)$ and $\widetilde{z}(\lambda)$ to approximate the tabulated values of the CMFs. The Euclidean distance in the CIE 1931 chromaticity diagram is shown between brackets in the last column of Table III, and it verifies $\|(x_c, y_c) - (\widetilde{x}_c, \widetilde{y}_c\| \leq 0.01$ for the six LED colors under evaluation. Besides, the step of the MacAdam ellipse is always below 4, which is the maximum value permitted by ANSI so that the human eye cannot perceive that color difference [26]. The step of the MacAdam ellipse has been computed with the aid of the *LED Color Calculator tool* provided by OSRAM [27], which employs the derivations presented in [28] and [29] for computing the MacAdam ellipses, interpolated from the original 25 ellipses identified by MacAdam in [30]. Besides, we illustrate the accuracy of the derived analytical expression in Fig. 4. Note that the actual and approximated points show negligible differences in positions.

C. Exact Power Allocation Method for any Tri-Color LED Combinations

Let us assume that LED chips with color indexes in set $\mathcal{C} = \{c_1, c_2, c_3\}$ are utilized to generate an aggregate spectrum

$$p_{\mathrm{o},\mathcal{C}}(\lambda|\mathbf{p}) = p_1 \frac{p_{\mathrm{o},c_1}(\lambda)}{I_{0,c_1}} + p_2 \frac{p_{\mathrm{o},c_2}(\lambda)}{I_{0,c_2}} + p_3 \frac{p_{\mathrm{o},c_3}(\lambda)}{I_{0,c_3}}, \quad (39)$$

where $\mathbf{p} = [p_1, p_2, p_3]^{\mathrm{T}}$ is a unit-norm vector that identifies the fraction of optical power that is allocated in each LED chip in set $\mathcal{C}$, i.e. $p_1 + p_2 + p_3 = 1$, and I_{0,c_1}, I_{0,c_2} and I_{0,c_3} are the normalization factors that make unitary the total optical power emitted by each color chip of the tri-color LED. Then, the tri-stimulus values of the aggregate optical spectrum can be formulated as

$$X_{\mathcal{C}}(\mathbf{p}) = p_1\left(\frac{X_{c_1}}{I_{0,c_1}} - \frac{X_{c_3}}{I_{0,c_3}}\right) + p_2\left(\frac{X_{c_2}}{I_{0,c_2}} - \frac{X_{c_3}}{I_{0,c_3}}\right) + \frac{X_{c_3}}{I_{0,c_3}}, \quad (40)$$

$$Y_{\mathcal{C}}(\mathbf{p}) = p_1\left(\frac{Y_{c_1}}{I_{0,c_1}} - \frac{Y_{c_3}}{I_{0,c_3}}\right) + p_2\left(\frac{Y_{c_2}}{I_{0,c_2}} - \frac{Y_{c_3}}{I_{0,c_3}}\right) + \frac{Y_{c_3}}{I_{0,c_3}}, \quad (41)$$

$$Z_{\mathcal{C}}(\mathbf{p}) = p_1\left(\frac{Z_{c_1}}{I_{0,c_1}} - \frac{Z_{c_3}}{I_{0,c_3}}\right) + p_2\left(\frac{Z_{c_2}}{I_{0,c_2}} - \frac{Z_{c_3}}{I_{0,c_3}}\right) + \frac{Z_{c_3}}{I_{0,c_3}}. \quad (42)$$

Then, the emitted aggregate white light spectrum can be finally matched into the CIE 1931 chromaticity diagram with the aid of the following two linear equations, i.e.,

$$x_{\mathcal{C}}(\mathbf{p}) = \frac{X_{\mathcal{C}}(\mathbf{p})}{X_{\mathcal{C}}(\mathbf{p}) + Y_{\mathcal{C}}(\mathbf{p}) + Z_{\mathcal{C}}(\mathbf{p})} = x_{\mathrm{L}}(T), \quad (43)$$

$$y_{\mathcal{C}}(\mathbf{p}) = \frac{Y_{\mathcal{C}}(\mathbf{p})}{X_{\mathcal{C}}(\mathbf{p}) + Y_{\mathcal{C}}(\mathbf{p}) + Z_{\mathcal{C}}(\mathbf{p})} = y_{\mathrm{L}}(T), \quad (44)$$

whose right-hand side terms are the (x, y) coordinates of the point of the Planckian locus that correspond to the target CCT value T, which are denoted by $x_{\mathrm{L}}(T)$ and $y_{\mathrm{L}}(T)$. Note that the Planckian locus contains the coordinates of the light sources that are interpreted as white light by the human eye and, due to that, they are uniquely characterized by the given CCT value. Cubic spline approximation for the coordinates of the Planckian locus in the CIE 1931 diagram is given by [31]

$$x_{\mathrm{L}}(T) = \begin{cases} -0.2661239\frac{10^9}{T^3} - 0.2343589\frac{10^6}{T^2} \\ +0.8776956\frac{10^3}{T} + 0.179910, & 1667 \leq T \leq 4000 \\ \\ -3.0258469\frac{10^9}{T^3} + 2.1070379\frac{10^6}{T^2} \\ +0.2226347\frac{10^3}{T} + 0.240390, & 4000 \leq T \leq 25000 \end{cases} \quad (45)$$

and

$$y_{\mathrm{L}}(T) = \begin{cases} -0.9549476x_{\mathrm{L}}^3(T) - 1.37418593x_{\mathrm{L}}^2(T) \\ +2.09137015x_{\mathrm{L}}(T) - 0.16748867, & 2222 \leq T \leq 4000 \\ \\ +3.0817580x_{\mathrm{L}}^3(T) - 5.87338670x_{\mathrm{L}}^2(T) \\ +3.75112997x_{\mathrm{L}}(T) - 0.37001483, & 4000 \leq T \leq 25000 \end{cases} \quad (46)$$

which is valid for our region of interest, which spans from a 2700 K (warm) to 6500 K (cool) aggregate emitted white light.

For the computation of the optical power allocation that is needed per color chip of the tri-color LED, to provide an aggregate white light with a target CCT value T, a system of two linear equations with two unknown variables (p_1, p_2) must be solved. Starting from this 2-by-2 linear system, it is possible to show that the *unknown* variables attain the form

$$p_1(T) = \frac{a_{2,2}(T)\, b_1(T) - a_{1,2}(T)\, b_2(T)}{a_{1,1}(T)\, a_{2,2}(T) - a_{1,2}(T)\, a_{2,1}(T)}, \quad (47)$$

$$p_2(T) = \frac{a_{1,1}(T)\, b_2(T) - a_{2,1}(T)\, b_1(T)}{a_{1,1}(T)\, a_{2,2}(T) - a_{1,2}(T)\, a_{2,1}(T)}, \quad (48)$$

where

$$a_{1,1} = \left(\frac{X_{c_1}}{I_{0,c_1}} - \frac{X_{c_3}}{I_{0,c_3}}\right) - x_{\mathrm{L}}(T)\left(\frac{X_{c_1}+Y_{c_1}+Z_{c_1}}{I_{0,c_1}} - \frac{X_{c_3}+Y_{c_3}+Z_{c_3}}{I_{0,c_3}}\right), \quad (49)$$

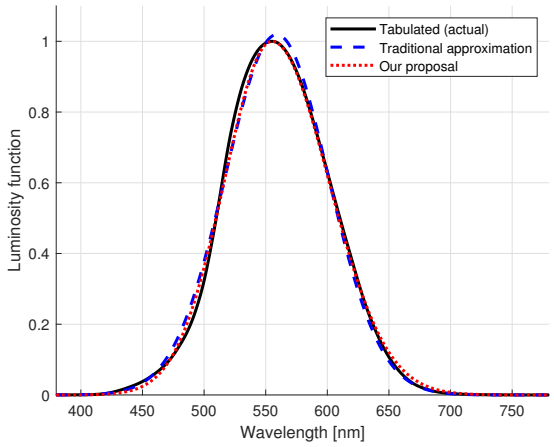

Fig. 5. Comparison of the actual (tabulated) luminous efficacy function $V(\lambda)$ with the traditional (symmetric) Gaussian formula and the new proposed asymmetric Gaussian approximation. As expected, the asymmetric Gaussian approximation $\widetilde{V}(\lambda)$ gives a more accurate fit for the tabulated values in $V(\lambda)$.

$$a_{1,2}=\left(\frac{X_{c_2}}{I_{0,c_2}}-\frac{X_{c_3}}{I_{0,c_3}}\right)-x_{\mathrm{L}}(T)\left(\frac{X_{c_2}+Y_{c_2}+Z_{c_2}}{I_{0,c_2}}-\frac{X_{c_3}+Y_{c_3}+Z_{c_3}}{I_{0,c_3}}\right), \tag{50}$$

$$a_{2,1}=\left(\frac{Y_{c_1}}{I_{0,c_1}}-\frac{Y_{c_3}}{I_{0,c_3}}\right)-y_{\mathrm{L}}(T)\left(\frac{X_{c_1}+Y_{c_1}+Z_{c_1}}{I_{0,c_1}}-\frac{X_{c_3}+Y_{c_3}+Z_{c_3}}{I_{0,c_3}}\right), \tag{51}$$

$$a_{2,2}=\left(\frac{Y_{c_2}}{I_{0,c_2}}-\frac{Y_{c_3}}{I_{0,c_3}}\right)-y_{\mathrm{L}}(T)\left(\frac{X_{c_2}+Y_{c_2}+Z_{c_2}}{I_{0,c_2}}-\frac{X_{c_3}+Y_{c_3}+Z_{c_3}}{I_{0,c_3}}\right), \tag{52}$$

$$b_1(T) \;=\; x_{\mathrm{L}}(T)\left(\frac{X_{c_3}+Y_{c_3}+Z_{c_3}}{I_{0,c_3}}\right)-\frac{X_{c_3}}{I_{0,c_3}}, \tag{53}$$

and

$$b_2(T) \;=\; y_{\mathrm{L}}(T)\left(\frac{X_{c_3}+Y_{c_3}+Z_{c_3}}{I_{0,c_3}}\right)-\frac{Y_{c_3}}{I_{0,c_3}}. \tag{54}$$

Once we get the optical power allocation per color chip of the tri-color LED, the luminous flux allocation can be easily computed using the luminous efficacy of radiation of each color chip, which is the ratio between the luminous flux [lm] and the optical power [W] and can be computed as

$$K_{\mathrm{v,e}}=\frac{\phi_{\mathrm{v},c}}{P_{\mathrm{opt},c}}=\frac{683.002\int_{380}^{780}V(\lambda)\,p_{\mathrm{o},c}(\lambda)\,\mathrm{d}\lambda}{\int_{380}^{780}p_{\mathrm{o},c}(\lambda)\,\mathrm{d}\lambda}, \tag{55}$$

where $V(\lambda)$ is the luminosity function that has been traditionally approximated as an scaled symmetric Gaussian function [32], i.e.,

$$V(\lambda)\approx 1.019\exp\Big\{-285.4\big(\lambda-0.559\big)^2\Big\}, \tag{56}$$

in which the value of λ should be plugged in micrometers (μm). However, in this paper we propose a better approximation, identifying the parameters of an asymmetric Gaussian function that matches best the tabulated $V(\lambda)$ function, i.e.,

$$\widetilde{V}(\lambda)=1.0\exp\left\{-\frac{276.5\,\big(\lambda-555\big)^2}{\big[1+0.18\,\mathrm{sign}(\lambda-0.555)\big]}\right\}, \tag{57}$$

where $\mathrm{sign}(x)$ equals 1 for $x\geq 0$ and -1 otherwise. Fig. 5 plots the tabulated, symmetric Gaussian approximation, and the proposed asymmetric Gaussian approximation for the $V(\lambda)$ function. The new asymmetric Gaussian approach gives a better fit than the traditional symmetric Gaussian one, reducing the root mean square (RMS) error from 0.0220 when using the *old* approximation in (56) to 0.0157 when using the *new* approximation in (57). In this way, it is also possible to compute the luminous flux of the aggregate white light in closed form.

IV. Results and Key Performance Analysis

After deriving the formulas that define in closed form the optical power to be allocated per color chip to obtain an aggregate white light at the target CCT, we are ready to assess the performance of few representative tri-color combinations. Without loss of generality, we consider the combination of Red-Green-Blue (RGB), Amber-Cyan-Blue (ACB), RedOrange-Cyan-Blue (ROCB), and RedOrange-Green-Blue (ROGB) tri-color LEDs, and we take LUXEON Rebel color LEDs as reference [33]. Then, using the equations derived in Section III-C, we compute the power allocation per chip in each of the tri-color LED combination under study for all the points in the Planckian locus of the CIE 1931 diagram. Note that the proposed method is valid to study the key performance metrics of any tri-color LED combination that may be used by a VLC system designer, even with single color LED chips provided by different manufacturers.

Fig. 6 depicts the power allocated per color LED when different tri-color LED combinations are taken into consideration to achieve the target white light color. In order to make fair comparisons, the overall optical transmit power is normalized in all the tri-color LED combinations under study (i.e., $P_{\mathrm{total}}=p_1+p_2+p_3=1$). For warm colors (low CCT), the Red, RedOrange, and Amber chips have more power allocated as the target color is closer to the red hue. However, when the power allocation per chip is changed to achieve a cooler aggregate white light (high CCT), the share of power among the three different individual colors tends to approach each other more evenly. These power allocations for each tri-color LED combination may generate different results in illumination and communication KPIs, even when the target CCT is the same. This is because each color chip of a tri-color LED has different characteristics in electrical-to-optical power conversion due to the materials that are used to convert electricity into light at different wavelengths (i.e., colors), as well as different luminous efficacy (i.e., luminous flux versus optical power ratio) due to the difference in sensitivity that the human eye has on different wavelengths within the visible light region of the optical spectrum.

The electrical and optical parameters of the six LUXEON Rebel color LEDs used in this paper are summarized in Table IV. Without loss of generality, we consider that the LED DC-bias point is $I_{\mathrm{DC}}=200\,\mathrm{mA}$ regardless of the LED

TABLE IV
ELECTRICAL AND OPTICAL PARAMETERS FOR THE SIX SAMPLE LUXEON REBEL COLOR LEDS USED TO CARRY OUT THE STUDIES OF THIS PAPER.

Color	Part No.	Typ. luminous flux ϕ_{v} @200mA [lm]	Typ. forward voltage V_{f} @200mA [V]	Luminous efficacy $K_{\mathrm{e,v}}$ [lm/W]	Optical transmit power P_{opt} @200mA [W]	$P_{\mathrm{opt}}/P_{\mathrm{elec}}$ @200mA [W/W]
Red (R)	LXM2-PD01-0040	29.18	1.98	167.19	0.1746	0.4408
RedOrange (RO)	LXM2-PH01-0060	40.74	1.98	242.57	0.1679	0.4241
Amber (A)	LXML-PL01-0050	32.83	2.58	418.29	0.0785	0.1521
Green (G)	LXML-PM01-0090	64.98	2.77	550.26	0.1181	0.2132
Cyan (C)	LXML-PB01-0070	50.46	2.77	358.93	0.1406	0.2538
Blue (B)	LXML-PB01-0023	18.59	2.77	78.86	0.2358	0.4256

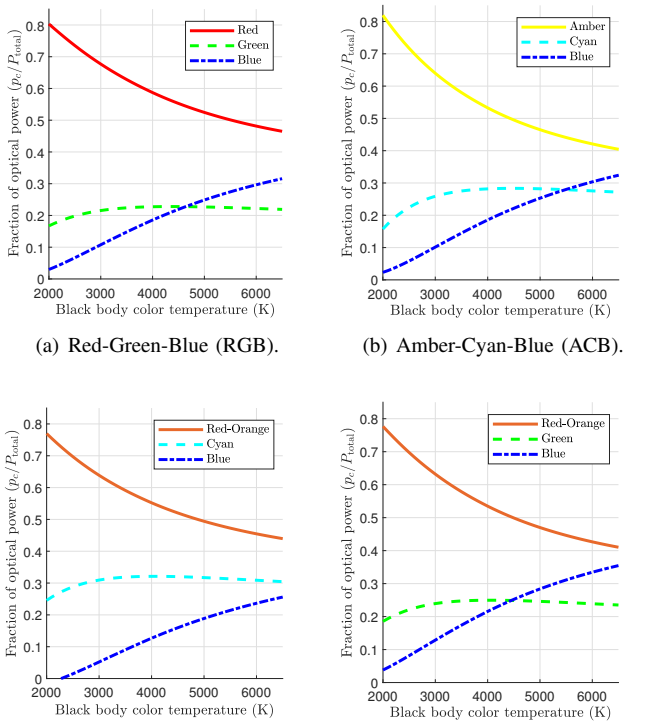

(a) Red-Green-Blue (RGB). (b) Amber-Cyan-Blue (ACB).

(c) RedOrange-Cyan-Blue (ROCB). (d) RedOrange-Green-Blue (ROGB).

Fig. 6. Power allocation per color chip for different tri-color LED combinations to achieve an aggregate white light at a target CCT in Kelvin (K). Total optical power is normalized (i.e., $P_{\mathrm{total}} = 1$) to make fair comparisons.

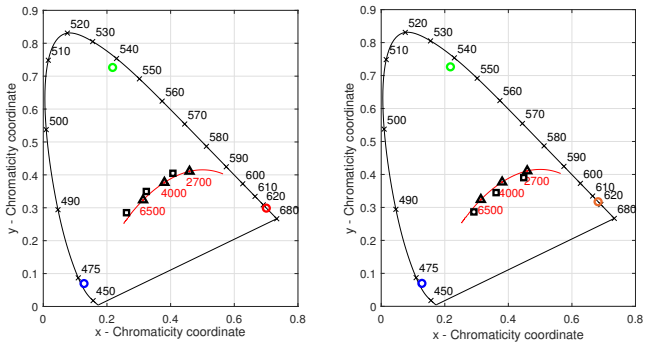

(a) Red-Green-Blue. (b) RedOrange-Green-Blue.

Fig. 7. CIE 1931 chromaticity coordinates for the aggregate (white) light when using RGB and ROGB tri-color LEDs. Square markers represent the coordinates when following *Method 1*, whereas triangle markers show the coordinates when using either *Method 2* or our new proposed method.

color under study. However, the forward voltage (V_{f}) at this same DC-bias point varies with the LED model because the materials that are used to build the different color LED chips are different. In addition, the optical power that is emitted per color LED also changes, as it depends on the electrical power (i.e., $P_{\mathrm{elec}} = V_{\mathrm{f}} \times I_{\mathrm{DC}}$) and the conversion efficiency of the color LED. Although we may use the information that appears in the data sheets of the color LED models to estimate the luminous efficacy ($K_{\mathrm{e,v}}$), we decided to compute this value ourselves in a more precise way by plugging the approximated spectral power emission (5) in (55), using for this purpose the parameters that were obtained from the measured spectral emission of each of these color LED models. Note that the green LED model presents the highest luminous efficacy as its emitted spectrum is centered in the region where the human eye is most sensitive, whereas the red and blue LED models have the lowest luminous efficacy because their spectra are located at both sides of the luminosity function (compare spectra for different LED colors in Fig. 2 and luminous efficacy function in Fig. 5). Data sheets of commercial LEDs usually provide information on the relative luminous flux of the device, which allows us to compute the optical transmit power for a forward current of $I_{\mathrm{DC}} = 200\,\mathrm{mA}$. Finally, we compute the ratio between optical power and electrical power as $P_{\mathrm{opt}}/(I_{\mathrm{DC}} \times V_{\mathrm{f}})$. Note that, if required, higher optical transmit powers can be obtained by aggregating multiple LED of the same type in transmission. Therefore, the derived analysis remains valid regardless of the size of the room that needs to be illuminated using tri-color LEDs.

A. Comparison with State-of-Art Power Allocation Methods

As an illustrative example, and without loss of generality, Fig. 7 shows the result of combining Red-Green-Blue (RGB) and RedOrange-Green-Blue (ROGB) Luxeon Rebel LED colors to get a warm (2700 K), neutral (4000 K) and cool (6500 K) white light on the CIE 1931 Planckian locus using two state-of-art methods (*Method 1*, *Method 2*) and our new proposed method. Table V shows the errors produced when each method is applied to obtain the target aggregate white light.

When considering the step size of the MacAdam ellipses and the Euclidean distance as metrics for the error evaluation [17], it is observed that *Method 1*, though widely used in the literature, does not provide an accurate result; this is because it can only *approximate* the three individual tristimulus values of each individual light source having as input only two chromaticity coordinates. In contrast, *Method 2* works extremely well; this is because the CIE 1931 (XYZ)

TABLE V
ERROR EVALUATION WHEN USING *Method 1*, *Method 2* AND THE NEW PROPOSED METHOD. ERROR IS MEASURED ACCORDING TO THE STEP-SIZE OF THE MACADAM ELLIPSE (EUCLIDEAN DISTANCE) OF TARGET AND ACTUAL CIE 1931 CHROMATICITY COORDINATES (x, y).

		2700 K	**4000 K**	**6500 K**
RGB	*Method 1*	30.5 (0.0525)	33.0 (0.0629)	32.5 (0.0648)
	Method 2	<0.5 (∼1e-6)	<0.5 (∼1e-9)	<0.5 (∼1e-5)
	Proposal	<0.5 (∼1e-6)	<0.5 (∼1e-9)	<0.5 (∼1e-5)
ROGB	*Method 1*	7.5 (0.0231)	11.5 (0.0370)	13.5 (0.0432)
	Method 2	<0.5 (∼1e-6)	<0.5 (∼1e-6)	<0.5 (∼1e-6)
	Proposal	<0.5 (∼1e-6)	<0.5 (∼1e-6)	<0.5 (∼1e-6)

color space has been deliberately designed such that the CMF $\bar{y}(\lambda)$ that is used to compute the tri-stimulus value Y of the light source is identical to the eye sensitivity function $V(\lambda)$, which is used to compute the corresponding luminous flux ϕ_{v}. Then, since there are two chromaticity coordinates and one tri-stimulus value as input in *Method 2*, it is possible to compute *exactly* the tri-stimulus values (X, Y, Z) of each of the three single-color light sources and, after that, determine the tri-stimulus values of the aggregate (white) light that is generated after the linear combination of three independent light sources.

Although *Method 2* is *exact*, it is based on illumination metrics, such as luminous flux and chromaticity coordinates of light sources, which may be cumbersome to determine in VLC systems. In such wireless communication systems, optical transmit power (or radiant flux) of the light source is a more important parameter to estimate the achievable data rate of the optical wireless link. The luminous flux of an LED, measured in lumen (lm), depends on the spectral emission of the light source, and its shape or profile varies with the LED junction temperature as shown in [17]. The same situation takes place with the CIE 1931 chromaticity coordinates (x, y) that are reported in the data sheets of commercial LEDs. Due to that, *Method 2* becomes unreliable as the input parameters depend strongly on the junction temperature at which each color chip of the tri-color LED is working. However, since our proposed optical power allocation method relies on the measured optical power spectrum of each single-color LED, its provided results are reliable regardless of the junction temperature and/or any other phenomenon that may affect the LED spectra.

B. Evaluation of the Illumination KPIs for a VLC System Using Different Tri-Color LED Combinations

We now study the most convenient tri-color LED combination to enable the largest luminous flux at the output per electrical unit power at the input as target KPI for illumination. To do so, we first compute the tri-stimulus values that correspond to each of the individual color chips that form the tri-color LED combination. We then compute the optical power allocation per color LED to reach the target CCT, using for this purpose the equations derived in Section III-C.

The performance of different tri-color LED combinations as function of the CCT of the aggregate white light that is generated is shown in Fig. 8. Note that the best tri-color LED combination in this case, regardless of the CCT that is aimed, is the RedOrange-Green-Blue (ROGB). This is

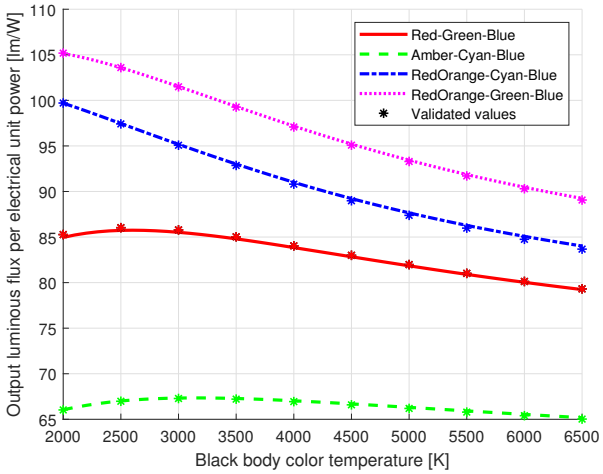

Fig. 8. Illumination performance for different tri-color LED combinations. Output luminous flux is presented for various target CCTs in Kelvin (K) when a unitary electrical power is allocated among the chips of the multi-color LED combination ($P_{\mathrm{elec}} = 1$ W). Validation results are also included in the form of point ('*') values.

justified by the high electrical-to-optical conversion efficiency ($P_{\mathrm{opt}}/P_{\mathrm{elec}}$) that characterizes RedOrange (RO) and Blue (B) LEDs, which makes this combination the most energy-efficient one for providing an aggregate white light using tri-color LED technology. Besides, the green color spectra in this tri-color LED combination is very sensitive to the human eye, which involves a large luminous efficacy and, as consequence, a large output luminous flux. Fig. 8 also includes point values that represent the detailed VLC system results that validate the theoretical formulas that have been derived in closed form. Whereas the results of the theoretical analysis are obtained with the approximated LED spectra proposed in [17] and the theoretical approximation of luminous efficacy function $\widetilde{V}(\lambda)$ proposed in Section III, validation results consider the actual single-color LED spectra measured with a spectrophotometer [17] and the actual tabulated values of the luminous efficacy function $V(\lambda)$. Note that the results obtained with the theoretical analysis derived here match very well the validated results based on the actual measurements of the LED spectra.

C. Evaluation of the Communication KPIs for a VLC System Using Different Tri-Color LED Combinations

For simplicity, we consider a fixed setup where both VLC transmitter and VLC receiver are positioned in front of each other, such that the angle of irradiance and angle of incidence are null (i.e., $\phi = \varphi = 0°$). Without loss of generality, we consider that the photodetector that is used in reception is the part number VTP4085H [34]. Note that similar results can be obtained with a different photodetector model, such as the one presented in [35], as black-silicon photodetectors show a similar responsivity behavior that grows linearly with the wavelength of the incident wave, with a peak responsivity value in the near infrared band. We also consider the visible light filter model FGS900 [36] to remove the optical interference coming from other adjacent optical frequency bands. Both photodetector responsivity and optical filter transmittance

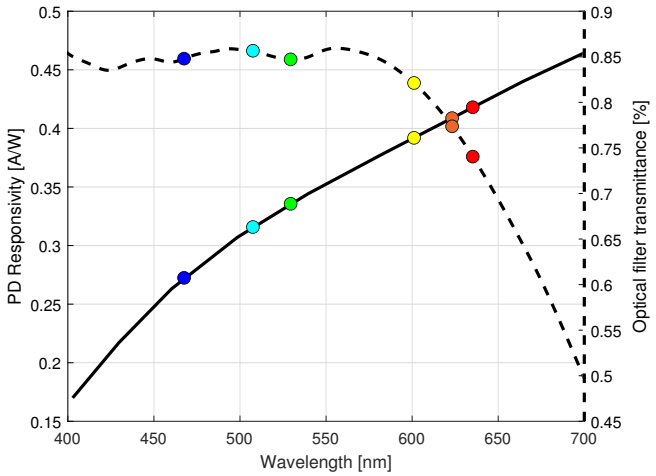

Fig. 9. Responsivity of photodetector VTP4085H (solid line) and transmittance of optical filter FGS900 (dashed line) used to evaluate the communication KPIs of a VLC system based on different tri-color LED combinations. Peak wavelengths $\lambda_{\mathrm{p},c}$ for all color LEDs are marked with circles.

are depicted in Fig. 9. The rest of the simulation parameters are summarized in Table VI.

The simulation results that assess the communications performance of a VLC system when using different tri-color LED combinations are summarized in Fig. 10. All these values have been computed considering a unitary total electrical transmit power. From these curves it is possible to see that ROCB is the most convenient tri-color LED combination at all CCT values, although RGB could potentially offer better performance at low CCTs (i.e., below 2000 K). The reason for this is that, at low CCT values (i.e., warm white light), a larger portion of the total optical power is allocated to the Red LED chip, and since the photodetector has higher responsivity in the red light region, the RGB combination is the most convenient. However, the transmittance of the visible light filter represented in Fig. 9 shows that the Red LED wavelengths are notably affected, which counteracts the good photodetector responsivity in that portion of the optical spectrum. As the CCT of the aggregate white light increases and its hue becomes cooler, the fraction of the optical power allocated to the Red LED chip decreases, and Green and Blue chips of the tri-color LED combinations gain relevance, degrading the communication performance of the VLC system. The ROCB combination experiences a similar phenomenon but, since the Cyan LED chip receives a higher allocated power as observed in Fig. 6(c), and a Cyan LED is also more energy efficient than a Green LED (see Table IV), it makes the ROCB combination outperform the RGB one when assessing the data communications KPI. Also, we would like to highlight that the use of Amber LED chips is not a good choice in tri-color LED combinations, neither in communications nor in illumination, due to its poor energy efficiency (see Table IV).

Finally, it is noted that the validation of results shown in Fig. 10 slightly differ from the ones obtained when using the closed form theoretical formulas derived in Section III. This minor difference in the values, but *not* in the shape of the curves, is due to the idealization of the actual visible

TABLE VI
SIMULATION PARAMETERS TO ASSESS THE COMMUNICATIONS PERFORMANCE (KPI) OF THE VLC SYSTEM.

Parameter	Description	Value	Unit
T_{abs}	Absolute temperature	300	[K]
R_{L}	Load resistance	50	[Ω]
F_{s}	Sampling frequency	10	[MHz]
$\phi_{1/2}$	Half-power semi-angle	60	[°]
d	Distance between LED and PD	2	[m]
A_{pd}	Active area of PD	21	[mm^2]

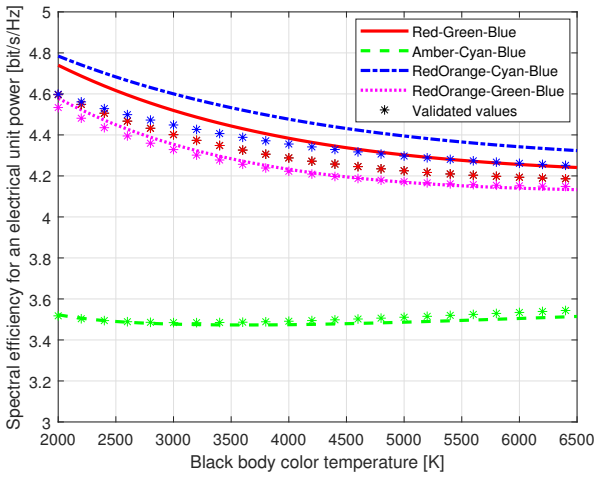

Fig. 10. Spectral efficiency of the VLC system versus target CCTs in Kelvin (K) for different tri-color LED combinations when a unitary electrical power is allocated among the three individual LED chips ($P_{\mathrm{elec}} = 1$ W). Validation results are also included in the form of point ('*') values.

light filter and photodetector responses used to obtained the closed-form results. That is, we considered an ideal optical filter with flat transmittance obtained as the average of actual transmittance values in the optical pass band of the FGS900 filter framed by the two most extreme peak wavelengths under study (i.e., between blue and read LED peak wavelengths), that is 0.837 nm, and a single value of the photodetector VTP4085H responsivity corresponding to the peak wavelength for each color LED. Validation results, in contrast, are obtained with tabulated actual values of both photodetector responsivity and optical filter transmittance.

D. Joint Evaluation of the Illumination and Communication KPIs

This section combines both illumination and communication performance by reformulating the optimization problem as a Pareto-optimal problem. We aim at maximizing both illumination and communication performance, as discussed in Section IV-B and Section IV-C, respectively. In this context, Fig. 11(a) shows the Pareto fronts for all the CCT of interest, where it can be observed that the combinations RGB and ACB are Pareto-dominated by ROGB and ROCB. However, both ROGB and ROCB are within the Pareto-front, which means that both of them can be considered as Pareto efficient.

To select a single tri-color LED combination that offers the best communication and illumination performance, we convert

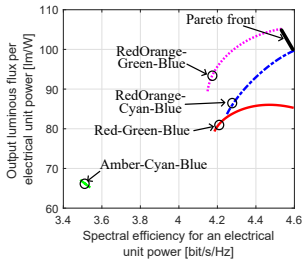

(a) Pareto fronts for different studied tri-color LED combinations.

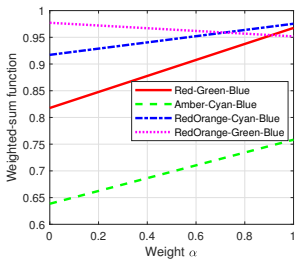

(b) Objective function vs. weight α for warm white (CCT = 2700 K).

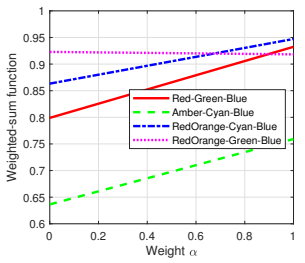

(c) Objective function vs. weight α for neutral white (CCT = 4000 K).

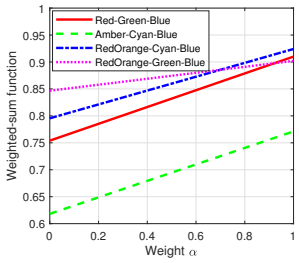

(d) Objective function vs. weight α for cool white (CCT = 6500 K).

Fig. 11. Representation of the best color combination to simultaneously maximize both illumination and communication metrics. In this sense, Pareto front for all CCT values and studied tri-color LED combinations is represented in (a), whereas values of the unique objective function to be maximized is represented in (b), (c) and (d) for warm (2700 K), neutral (4000 K) and cool (6500 K) white light, respectively.

the multi-objective optimization problem into an equivalent problem with a unique objective function to be maximized, by using the following weighted sum method:

$$f = \alpha\, C + (1-\alpha)\, I, \tag{58}$$

where $\alpha \in [0,1]$ is the weight that is defined by the decision maker, and C and I are the normalized spectral efficiency for an electrical unit power and the normalized optimum luminous flux per electrical unit power, respectively; that is, C and I are the communication and illumination metrics to be maximized, respectively. However, we are not looking for the best tri-color LED combination and CCT that provides the optimal performance for both communications and illumination, but we are rather interested in the multi-color LED combination that offers the best performance in both communications and illumination for each CCT, since the hue of the white light emitted by a VLC system is chosen by the user depending on its interests. Thus, the system presents two variables to be tuned, which are the weight α and the CCT and can be selected depending on the task that is prioritized (i.e., either communication or illumination) or the user comfort.

Figs. 11(b), 11(c) and 11(d) show the value of the weighted sum f in (58) for the three different CCT values under study when varying the value of weight α in its whole range. The results show that for most of the values of α (i.e., when $0 < \alpha \lesssim 0.7$), the ROGB combination offers the best joint communications and illumination performance for any CCT value, whereas the ROCB combination offers the best joint performance at higher values of α for any CCT. These results give the following insight: depending on the priority that the VLC system is expected to give for the communication and illumination services, which is modelled in this example by the value that the weighting coefficient α takes, the CCT to be configured by the user does not have a notable effect; that is, the configuration of the VLC system can be done beforehand with one specific type of tri-color LED, which could be either ROGB or ROCB depending on the services that wants to be prioritized, i.e., illumination or communications, respectively.

V. Conclusion

This paper introduced a new method to allocate the optical power among the color chips of any tri-color LED combination, beyond RGB LEDs, to provide VLC services while guaranteeing an aggregate white light at different target CCT values that is suitable for illumination. Unlike state-of-art solutions reported in the literature for optical power allocation in tri-color LEDs, this method is presented in closed form from the beginning. The derived expressions can be used to determine the tri-stimulus values of the aggregate white light produced by *any* combination of three color chips in tri-color LEDs, opening the door to new theoretical studies. As this method follows up the pre-defined steps to compute the CIE 1931 chromaticity coordinates of a light source, starting from the approximation of the LED emitted spectra $p_{\mathrm{o}}(\lambda)$, continuing with the computation of the tri-stimulus values (X, Y, Z), and finalizing with the determination of the (x, y) coordinates, the error produced when compared to the numerical computation with tabulated functions is negligible. Moreover, it was shown that, although white light at different CCT can be obtained with various tri-color LED combinations, the most energy-efficient one varies according to the target service KPI to be optimized. That is, RedOrange-Green-Blue (ROGB) is the most convenient tri-color LED combination for energy-efficient illumination in the whole white light palette (i.e., from low/warm to high/cool white light CCTs), whereas the tri-color LED combination with best spectral efficiency for communications is RedOrange-Cyan-Blue (ROCB).

Acknowledgment

This work was funded by the European Union under the Marie Sklodowska-Curie grant agreement No 101061853 and is based upon work from COST Action NEWFOCUS CA19111, supported by COST (European Cooperation in Science and Technology).

References

[1] L. Hanzo, H. Haas, S. Imre, D. O'Brien, M. Rupp, and L. Gyongyosi, "Wireless myths, realities, and futures: from 3G/4G to optical and quantum wireless," *Proc. IEEE*, vol. 100, no. Special Centennial Issue, pp. 1853–1888, May 2012.

[2] Q. Wang, Z. Wang, and L. Dai, "Asymmetrical hybrid optical OFDM for Visible Light Communications with dimming control," *IEEE Photon. Technol. Lett.*, vol. 27, no. 9, pp. 974–977, 2015.

[3] Y. Wu, Z. Wang, T. Mao, and J. Chen, "Chromaticity-domain index modulation for visible light communication," in *Proc. International Conference on Optoelectronic and Microelectronic Technology and Application*, J. Liu, Ed., vol. 11617, International Society for Optics and Photonics. SPIE, 2020, p. 116173Y.

[4] A. Dowhuszko, M. Ilter, P. Pinho, R. Wichman, and J. Hämäläinen, "Effect of the color temperature of LED lighting on the sensing ability of visible light communications," in *Proc. IEEE Int. Conf. Commun. Workshops*, June 2021, pp. 1–6.

[5] Y. Wang, L. Tao, X. Huang, J. Shi, and N. Chi, "8-Gb/s RGBY LED-based WDM VLC system employing high-order CAP modulation and hybrid post equalizer," *IEEE Photon. J.*, vol. 7, no. 6, pp. 1–7, Dec. 2015.

[6] H. Chun, S. Rajbhandari, G. Faulkner, D. Tsonev, E. Xie, J. McKendry, E. Gu, M. Dawson, D. O'Brien, and H. Haas, "LED based wavelength division multiplexed 10 Gb/s visible light communications," *J. Lightw. Tech.*, vol. 34, no. 13, pp. 3047–3052, July 2016.

[7] B. Genovés Guzmán, A. Dowhuszko, V. Gil Jiménez, and A. Pérez-Neira, "Cooperative transmission scheme to address random orientation and blockage events in VLC systems," in *Proc. Int. Symp. Wireless Commun. Systems*, Aug 2019, pp. 351–355.

[8] B. Genovés Guzmán, A. Dowhuszko, V. Gil Jiménez, and A. Pérez-Neira, "Resource allocation for cooperative transmission in optical wireless cellular networks with illumination requirements," *IEEE Trans. Commun.*, vol. 68, no. 10, pp. 6440–6455, Oct. 2020.

[9] Y. Zuo and J. Zhang, "Energy-efficient optimization design for the multi-color LED based visible light communication systems under illumination constraints," *Appl. Sci.*, vol. 9, no. 1, pp. 1–14, Dec. 2018.

[10] Y. Zuo, J. Zhang, and J. Qu, "Power allocation optimization design for the quadrichromatic LED based VLC systems with illumination control," *Crystals*, vol. 9, no. 3, pp. 1–13, Mar. 2019.

[11] S. Lou, C. Gong, N. Wu, and Z. Xu, "Power optimization under brightness and communication requirements for visible light communication based on MacAdam ellipse," *J. Commun. Inf. Netw.*, vol. 2, no. 4, pp. 28–35, Dec. 2017.

[12] R. Jiang, Z. Wang, Q. Wang, and L. Dai, "Multi-user sum-rate optimization for visible light communications with lighting constraints," *J. Lightw. Tech.*, vol. 34, no. 16, pp. 3943–3952, Aug. 2016.

[13] C. Gong, S. Li, Q. Gao, and Z. Xu, "Power and rate optimization for visible light communication system with lighting constraints," *IEEE Trans. Signal Process.*, vol. 63, no. 16, pp. 4245–4256, Aug. 2015.

[14] *IEEE Standard for Local and metropolitan area networks–Part 15.7: Short-Range Optical Wireless Communications*, IEEE SA, 2018.

[15] D. Karunatilaka, V. Kalavally, and R. Parthiban, "Improving lighting quality and capacity of OFDM-based WDM-VLC systems," *IEEE Photon. Technol. Lett.*, vol. 28, no. 20, pp. 2149–2152, Oct. 2016.

[16] W. Gunawan, Y. Liu, C.-W. Chow, Y.-H. Chang, C.-W. Peng, and C.-H. Yeh, "Two-level laser diode color-shift-keying orthogonal-frequency-division-multiplexing (LD-CSK-OFDM) for optical wireless communications," *J. Lightw. Tech.*, vol. 39, no. 10, pp. 3088–3094, May 2021.

[17] A. Dowhuszko and B. Genovés Guzmán, "Closed form approximation of the actual spectral power emission of commercial color LEDs for VLC," *J. Lightw. Tech.*, vol. 40, no. 13, pp. 4311–4320, July 2022.

[18] B. G. Guzman, J. Talavante, D. F. Fonseca, M. S. Mir, D. Giustiniano, K. Obraczka, M. E. Loik, S. Childress, and D. G. Wong, "Toward sustainable greenhouses using battery-free LiFi-enabled Internet-of-Things," *IEEE Commun. Mag.*, vol. 61, no. 5, pp. 129–135, May 2023.

[19] CIE, *Commission internationale de l'Eclairage proceedings, 1931*. Cambridge University Press, 1932.

[20] G. Wyszecki and W. S. Stiles, *Color Science: Concepts and Methods, Quantitative Data and Formulae*, 2nd ed. New York: John Wiley and Sons, 2000.

[21] E. Schubert, *Light-Emitting Diodes*, 2nd ed. Cambridge University Press, 2006.

[22] C. Wyman, P. Sloan, and P. Shirley, "Simple analytic approximations to the CIE XYZ color matching functions," *J. Computer Graphics Techniques*, vol. 2, no. 2, pp. 1–11, July 2013.

[23] A. Dowhuszko and A. Pérez-Neira, "Achievable data rate of coordinated multi-point transmission for visible light communications," in *Proc. IEEE Int. Symp. Personal, Indoor, and Mobile Radio Commun.*, Oct. 2017, pp. 1–7.

[24] J.-B. Wang, Q.-S. Hu, J. Wang, M. Chen, and J.-Y. Wang, "Tight bounds on channel capacity for dimmable visible light communications," *J. Lightw. Tech.*, vol. 31, no. 23, pp. 3771–3779, Dec. 2013.

[25] I. Gradshteyn and I. Ryzhik, *Table of Integrals, Series, and Products*, 7th ed. Academic Press, New York, 2007.

[26] "American National Standard for Electric Lamps– Specifications for the Chromaticity of Fluorescent Lamps," American National Standards Institute (ANSI), Rosslyn, VA, Standard, Dec. 2014.

[27] OSRAM, "LED ColorCalculator," [Online]. Available: https://www.osram.us/cb/tools-and-resources/applications/led-colorcalculator/index.jsp .

[28] K. Chickering, "Optimization of the MacAdam-modified 1965 friele color-difference formula," *J. Opt. Soc. Am.*, vol. 57, no. 4, pp. 537–541, Apr. 1967.

[29] ——, "FMC color-difference formulas: Clarification concerning usage," *J. Opt. Soc. Am.*, vol. 61, no. 1, pp. 118–122, Jan. 1971.

[30] D. L. MacAdam, "Visual sensitivities to color differences in daylight," *J. Opt. Soc. Am.*, vol. 32, no. 5, pp. 247–274, May 1942.

[31] K. Young-Sun, C. Bong-Hwan, K. Bong-Soon, and H. Doo-Il, "Color temperature conversion system and method using the same," Patent US7 024 034B2, 2006.

[32] J. Palmer, *Radiometry and photometry: Units and conversions, Handbook of Optics Part III,*, 2nd ed., M. Bass, Ed. New York: McGraw-Hill, 2001.

[33] Lumileds, "LUXEON Rebel color line — High flux and efficacy on industry's most widely used color LED platform," Nov. 2017.

[34] "Excelitas Technologies VTP4085H - Si PD, Ceramic, 21mm2," https://www.excelitas.com/product/vtp4085h-si-pd-ceramic-21mm2?filename=Excelitas%20VTP4085H%20datasheet.pdf, Accessed: 2024-2-18.

[35] A. Dowhuszko, M. Ilter, and J. Hämäläinen, "Visible light communication system in presence of indirect lighting and illumination constraints," in *Proc. IEEE Int. Conf. Commun.*, June 2020, pp. 1–6.

[36] "Thorlabs FGS900 - 25 mm KG3 Colored Glass Bandpass Filter, 315 - 710 nm ," https://www.thorlabs.com/thorproduct.cfm?partnumber=FGS900, Accessed: 2024-2-18.